Sustainable Energy & Fuels

Accepted Manuscript

This article can be cited before page numbers have been issued, to do this please use: M. Szri, B. R. Giri, Z. Wang, A. E. Dawood, B. Viskolcz and A. Farooq, *Sustainable Energy Fuels*, 2018, DOI: 10.1039/C8SE00207J.

ROYAL SOCIETY OF CHEMISTRY

rsc.li/sustainable-energy

View Article Online
DOI: 10.1039/C8SE00207J

Glycerol Carbonate as Fuel Additive for Sustainable Future

Milán Szőri[1], Binod Raj Giri*[,2], Zhandong Wang[2], Alaaeldin E. Dawood[2], Béla Viskolcz[1], Aamir Farooq*[,2]

[1] Institute of Chemistry, Faculty of Materials Science and Engineering, University of Miskolc, Egyetemváros A/4., H-3515 Miskolc, Hungary
[2] King Abdullah University of Science and Technology (KAUST), Clean Combustion Research Center, Physical Sciences and Engineering Division, Thuwal 23955-6900, Saudi Arabia

*Corresponding Author - Email: Binod.Giri@kaust.edu.sa; Aamir.Farooq@kaust.edu.sa

View Article Online
DOI: 10.1039/C8SE00207J

Abstract

Policy-makers and researchers have been considering a shift from conventional fossil fuels to renewable sources due to the growing concerns over global warming and diminishing oil reserves. Biodiesel, a renewable bio-drive fuel, can be derived from vegetable oils and animal fats, and is considered to be bio-degradable, non-toxic and environmentally friendly. Cetane number and caloric power of biodiesel are quite similar to those of conventional diesel. Crude glycerol of about 10-20% by volume appears as a byproduct in biodiesel production. Increasing demand of biodiesel has led to a substantial increase of glycerol supply in the global market, and dramatic fall in the price of glycerol which has warranted alternative uses of glycerol. One potential way to deal with crude glycerol overflow is to convert it to glycerol carbonate (GC) and use GC as a fuel or fuel additive. Prior studies have indicated that carbonate esters can significantly reduce particulate emissions during engine combustion. In this work, we have explored possible reaction pathways in the initial stage of glycerol carbonate pyrolysis. *Ab Initio*/RRKM-master equation methods are employed to differentiate various reaction pathways, and to obtain pressure- and temperature- dependence of the major channels. We have found that glycerol carbonate decomposes almost exclusively to produce CO_2 and 3-hydroxypropanal over 800 – 2000 K, and radical forming channels are unimportant. As 3-hydroxypropanal is one of the main products of GC decomposition, and aldehydes are known to have a very high impact on soot reduction, we conclude that GC can have a great potential for cleaner combustion as a fuel additive.

Keywords: *Biofuels; Glycerol carbonate; Clean Combustion; Ab initio/RRKM-Master equation; Unimolecular reaction.*

View Article Online
DOI: 10.1039/C8SE00207J

1. Introduction

Over the last decade or so, concerns over global warming and diminishing petroleum reserves have continued to rise. Transportation driven by traditional fossil fuels contributes significantly towards CO_2 emissions. Such concerns have led to concentrated efforts directed at shifting from conventional fuels to renewable alternatives that can promote cleaner combustion by reducing greenhouse gases and particulate matters. European Union "20/20/20" put mandatory goals for 2020 to reduce the greenhouse gas emissions by 20% compared to 1990, improve energy efficiency by 20% compared to the forecasts for 2020, and make the renewable energy share to be 20% to the total European energy mix.[1] Bio-derived fuels come with fuel-born oxygen, e.g., 10.8% in rapeseed methyl ester. Fuel-born oxygen is very effective in reducing the formation and growth of soot nuclei.[2] Some studies have even shown that fuel-born oxygen of 30% or more by weight can make the combustion process to go smokeless.[3-5] The goals of cleaner combustion have encouraged more production of biofuels on a large scale worldwide. Among bio-derived fuels, biodiesel stands out from health and environmental prospective because i) these are low in sulfur content, ii) these emit low level of hydrocarbons and CO, iii) these are bio-degradable and non-toxic, iv) these have high cetane number and caloric power similar to that of fossil fuels.[6] Biodiesel can be derived from vegetable oils and animal fats via industrial processes of esterification or transesterification. During biodiesel production, crude glycerol of 10-20% by volume is formed as a byproduct. Increasing use of biodiesel has led to a substantial increase of glycerol supply in the global market. This recently led to a dramatic fall of glycerol price, reaching the lowest historic value (3-5 cents a pound of glycerol).[6] The low price and huge surplus of glycerol warrants explorations of its alternative uses to make value-added products and to reduce the impacts of disposal. A recent review article by Rodrigues et al.[7] highlights the three possible ways to upgrade glycerol into value-added chemical feedstocks.

View Article Online
DOI: 10.1039/C8SE00207J

One feasible way to deal with crude glycerol overflow is its direct use as a fuel or fuel additive. However, high viscosity (1487 mPa·s at 293 K), high melting point (m.p=18.7 °C) and high auto-ignition temperature (370 °C) of glycerol has limited its application as fuel or additive, and also the presence of mineral salts causes corrosion in engines.[6] Instead, conversion of glycerol into value-added chemicals has received much attention.[7-10] One promising process is to convert glycerol into glycerol carbonate (GC) with relatively high yield. For example, Ochoa-Gómez et al. [11, 12] investigated the synthesis of glycerol carbonate from transesterification of glycerol and dimethyl carbonate. They achieved ~100% conversion and 95% yield in 90 mins at a temperature of 95 °C.[12] Very recently, Khandey et al.[9] reported a transesterification pathway to convert glycerol into glycerol carbonate by using Lithium-oil palm ash zeolite (Li-OPAZ) catalyst. They were able to achieve a very high yield ~98.1% of glycerol carbonate with 100% glycerol conversion in 90 mins under optimal condition of 343 K, dimethyl carbonate to glycerol molar ratio of 2, and 2 % by weight of the catalyst load. There are other chemical routes for the synthesis of glycerol carbonate by utilizing CO_2; and some of them look very promising to be applied in industrial scale.[10] Glycerol carbonate is water-soluble, nontoxic, viscous (85.4 mPa·s at 298 K), and has melting point (m.p = -69 °C), auto-ignition temperature of 404°C, high oxygen content (59% of oxygen by weight and O:C ratio of 1). Moreover, it is renewable [11], and can be a good candidate to sequester CO_2 as a chemical feedstock for sustainable future. Previous studies on carbonate esters [13, 14] have shown that such oxygenated fuels can significantly reduce unburnt hydrocarbons, CO and particulate matter emissions. However, the effectiveness of oxygenated fuel additives depends on the structure/size of the additive molecule, and a key controlling factor is the oxygen content of the molecule.[15, 16] The properties of glycerol carbonate, therefore, make it a very promising fuel additive for clean combustion by ensuring

View Article Online
DOI: 10.1039/C8SE00207J

the sustainability of future internal combustion engines.

However, efficient utilization of glycerol carbonate (GC) as a biofuel or fuel additive requires detailed understanding of the kinetic behavior of GC to accurately predict combustion behavior and emissions. To the best of our knowledge, there are no data available in the literature describing the combustion/pyrolysis kinetics of GC. Even though, one can speculate that glycerol carbonate may decompose via C-C and C-O bond scissions as seen in cyclic compounds (e.g., cyclopentane [17], cyclohexane [17, 18], methylcyclohexane [19], pyrrolidine [20], tetrahydrofuran [21] and 1,4-dioxane [22]). The resulting radicals may further react to produce a wide spectrum of oxygenated compounds. Besides radical forming pathways, molecular channels eliminating H_2, H_2O, CO, CO_2, and CH_2O are also feasible (see Fig. 1S of Supplementary Material for the reaction scheme). These oxygenated intermediates and/or products of glycerol carbonate decomposition may effectively alter the low-temperature chemistry and may help cleaner burning. This work aims to explore various possible reactions of glycerol carbonate, particularly the initial steps of pyrolysis, and to rationalize the pressure- and temperature- dependence of the rate coefficients using high level *ab initio*/RRKM-master equation calculations.

2. Computational Details

***Ab Initio* Calculations.** At first, Gaussian-4 theory (G4)[23] was employed to explore the possible reaction pathways of glycerol carbonate (GC, 4-(hydroxymethyl)-1,3-dioxolan-2-one). Intrinsic reaction coordinate (IRC) calculations[24, 25] with a step size of 0.06 a.u. were carried out by employing B3LYP functional[26, 27] using Pople's split-valence 6-31G(2df,p) Gaussian basis set[28]. These calculations ensured that the reaction pathways originating from the transition states led to the appropriate minima. Low-energy reaction pathways were identified at the G4 level of theory, and then these were selected for re-optimization at the

View Article Online
DOI: 10.1039/C8SE00207J

second-order Møller–Plesset (MP2)[29] perturbation theory using Dunning's triple-ς basis set (cc-pVTZ) [30] applying the "tight" convergence criterion. The optimized structures were further characterized by normal mode analysis to distinguish their identity on the PES. The MP2/cc-pVTZ harmonic vibrational frequencies were scaled[31] by a factor of 0.95 and these were used for the calculations of thermodynamic properties and rate coefficients.

The reliability of the calculated rate coefficients depends strongly upon the accuracy of the energy barriers. Therefore, the energetics of glycerol carbonate decomposition were refined by performing single-point coupled-cluster calculations with single and double excitations[32-34] including the perturbative treatment of triple excitations (CCSD(T)).[35] As done in our previous studies[36-38], a two-point extrapolation scheme of Helgaker[39] was employed to obtain CCSD(T) energies at the complete basis set limit (CBS) by using cc-pVXZ (X = D, T, Q)[30, 40] basis sets. Such extrapolation scheme manifests into a high level energetic description (CCSD(T)/cc-pVXZ(X = D, T, Q)//MP2/cc-pVTZ) of the reaction of glycerol carbonate. Here, the Hartree-Fock limit (E_{HF}^{∞}) was obtained by applying Feller three-point exponential extrapolation [41] according to $E_{\mathrm{HF}}(X) = E_{HF}^{\infty} + b \exp(-cX)$ using cc-pVXZ (X = D, T, Q, 5, 6) basis sets[42, 43]. This method culminates into three Hartree-Fock energies at the infinite basis set limit (E_{HF}^{∞}) *viz.* HF/cc-pV(D,T,Q)Z, HF/cc-pV(T,Q,5)Z and HF/cc-pV(Q,5,6)Z. As for the correlation energy, two point extrapolation of the form $E_{corr}(X) = E_{corr}^{\infty} + b'X^{-3}$ was used, where X was either 2 and 3 or 3 and 4 for cc-pV(D,T)Z and cc-pV(T,Q)Z basis sets, respectively. Finally, CCSD(T) energies at the infinite basis set limit, *i.e.,* CCSD(T)/cc-pV(D,T)Z or CCSD(T)/cc-pV(T,Q)Z were obtained by adding E_{HF}^{∞} and E_{corr}^{∞} together. Frozen core approximation was applied for all CCSD(T) calculations. To assess the contribution of higher excitations, T_1 diagnostics[44] were computed. The largest T_1 diagnostic value was 0.0223 for one of the transition states (TS1b, see Figure 3 below) at the CCSD(T)/cc-pVQZ level of theory. This value of T_1 may reveal the importance of non-

View Article Online
DOI: 10.1039/C8SE00207J

dynamical electron correlation effects.[44] For all other species, T_1 diagnostic values suggest that single reference methods applied here are adequate for accurate energetic description of the reactions of glycerol carbonate. All electronic structure calculations were performed by using Gaussian 09 program package.[45]

RRKM/Master Equation Calculations. In this work, ChemRate Master Equation (ME) code[46] was used to compute the pressure- and temperature- dependent rate coefficients, $k(T, p)$, for the unimolecular decomposition of GC at p = 0.01 – 100 atm and T = 800 – 2000 K. Master equation describes the temporal evolution of the energy- and time- dependent population of each species in a chemical system. The internal-energy-dependent master equation (1D-ME) can be written in the following form:

$$\frac{dy(E,t)}{dt} = F(E,t) + \omega \int_0^\infty [P(E,E')y(E',t) - P(E',E)y(E,t)]dE' - \sum_{i=1}^{channels} k_i(E)y(E,t) \quad (1)$$

where, $y(E,t)\mathrm{d}E$ is the time-dependent concentration of a chemical species with active energy in the range between E and $E + \mathrm{d}E$; ω is the collision frequency with the bath gas; $P(E, E')$ is the collisional energy transfer probability which takes the chemical species with energy in the range E' to $E'+\mathrm{d}E'$ to a new energy state between E and $E + \mathrm{d}E$; $F(E, t)\mathrm{d}E$ is the source term (e.g. chemical or photoactivation) describing the production of the chemical species in the energy range between E and $E + \mathrm{d}E$. The last term on the right-hand side of Eq. (1) accounts for the total rate of reaction *via* all possible channels; $k_i(E)$ is the energy-dependent unimolecular rate constant for decomposition reaction *via* the ith channel. $k_i(E)$ used in Eq. (1) was calculated using Rice-Ramsperger-Kassel-Marcus (RRKM) statistical rate theory [47-49]:

View Article Online
DOI: 10.1039/C8SE00207J

$$k(E) = L^{\neq} \frac{1}{h} \frac{G^{\ddagger}(E-E_0)}{\rho(E)} \quad (2)$$

where $L^{\neq}$ is the reaction path degeneracy; h is Planck's constant; $G^{\ddagger}(E - E_0)$ is the sum of states of the transition state; $\rho(E)$ is the density of states of reactant and E_0 is the reaction critical energy.

Eq. (1) can be written in a matrix form as given by Eq. (3) by replacing continuous functions with vectors. To do so, the energy axis is divided into a large number of small energy "bins" or "energy grains" of the size δE to construct energy-grained master equation.

$$\frac{d}{dt}\boldsymbol{y} = \boldsymbol{B}\boldsymbol{y} + \boldsymbol{F} \quad (3)$$

where $\boldsymbol{y}$ is the population vector with elements y_i and $\boldsymbol{B}$ is a square matrix that includes the elements of transition probabilities and micro-canonical rate coefficients. The vector ($\boldsymbol{F}$) describing the source term is removed for thermally activated system. The solution can be obtained by using an eigenvector-eigenvalue analysis. The lowest eigenvalue, *i.e.,* the largest negative eigenvalue of the matrix $\boldsymbol{B}$ equals to the overall thermal reaction rate coefficient ($k(T,p)$). For $k(T,p)$ calculations, energy grains (δE) of 50 cm^{-1} was used; whereas a smaller energy grain size of 5 cm^{-1} was used to compute sums and density of states and micro-canonical rate constants, $k(E)$. Sums and density of states were computed within rigid rotor and harmonic oscillators approximation using Beyer-Swinehart algorithm.[50] These computations utilized the calculated molecular parameters (vibrational frequencies and rotational constants) which are listed in the Supplementary Materials. Quantum mechanical tunneling correction was included in $k(E)$ for RRKM calculations. The energy-dependent tunneling transition probablility $\kappa(E)$ was calculated using the Eckart formula.[51] The characteristic length, barrier width (l), of the 1-D Eckart function for the potential energy profile along the reaction coordinate was obtained using the analytical expression reported by Johnston and Heicklen.[52] Reaction path degeneracies, $L^{\neq}$, were calculated using rotational

View Article Online
DOI: 10.1039/C8SE00207J

symmetry numbers and number of optical stereoisomers according to the formula provided by Gilbert and Smith.[47] In all cases, $L^{\neq}$ were found to be equal to 1. The rates of collisional energy transfer per downward collision were modeled using the single exponential down model with $\langle\Delta E\rangle_{down} = 0.55\ T\ K^{-1}\ cm^{-1}$. This functional form for energy transfer parameter, $\langle\Delta E\rangle_{down}$, delivers similar values in the temperature range of our interest as $\langle\Delta E\rangle_{down} = 200 \times (T/300)^{0.85}\ cm^{-1}$; the latter expression was used for other chemical systems of comparable size.[53-55] Argon was used as the collider gas and the bimolecular rate coefficients for collisions between argon and glycerol carbonate were calculated using Lennard-Jones (LJ) collision parameters. The LJ parameters used were $\sigma = 3.47$ Å and $\varepsilon/k_b = 114$ K for Ar [56], and $\sigma = 5.425$ Å and $\varepsilon/k_b = 485$ K for glycerol carbonate which is based on JetSurf 2.0 database for $C_6H_4O_2$ species.

3. Results and Discussion

Potential Energy Surface and Thermodynamic Properties. To discriminate among reaction channels, all possible reaction pathways on the potential energy surface (PES) of glycerol carbonate were considered (see reaction scheme, Fig. 1S, in the Supplementary Materials). As described earlier, G4 level of theory was used to map out the PES. It was found that simple bond fission reactions via C(O)-O bond or O-C and C-C bonds of glycerol carbonate producing open chain di-radicals have threshold energy of at least 340 kJ/mol. As can be seen in Fig. 1, C-H bond dissociation energy of methylene in $–CH_2OH$ is the least (BDE_0 = 387.3 kJ/mol) among all C-H bonds of GC. The elimination of hydroxylmethyl ($•CH_2OH$) radical via C-C bond fission of GC is found to have the lowest threshold energy (BDE_0 = 356.3 kJ/mol). These simple bond fission reactions are unlikely to occur as their threshold energies are very high as compared to the efficient molecular channels, such as CO_2 or H_2O elimination from GC via concerted mechanism, as will be discussed subsequently.

View Article Online
DOI: 10.1039/C8SE00207J

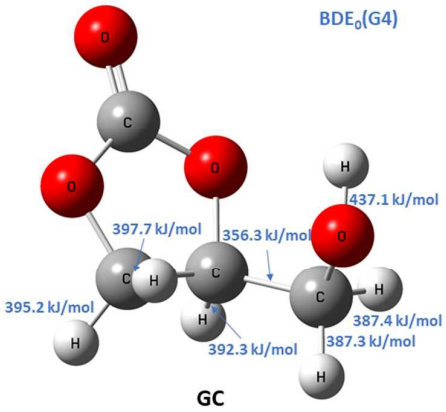

Figure 1. Calculated G4 bond dissociation energies at 0 K (BDE_0) for glycerol carbonate (GC)

Other molecular channels, such as elimination of H_2 and CH_2O, lie energetically very high ($E_0 \geq 400$ kJ/mol), and these proceed *via* tight transition states. So, these channels are also kinetically irrelevant. Consequently, GC primarily decomposes *via* the following three major energetically low-lying channels.

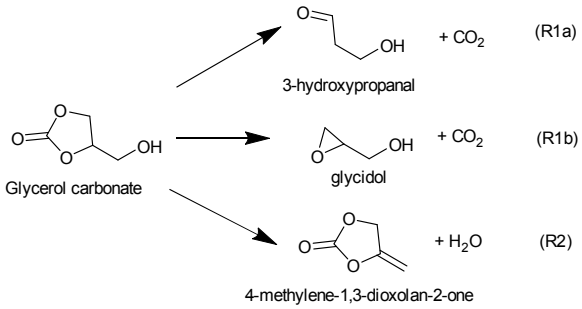

Figure 2. Major reaction pathways for the decomposition of glycerol carbonate (GC).

Both reactions, R1a and R1b, eliminate CO_2 to produce 3-hydroxypropanal and glycidol, respectively. However, the two mechanisms are quite different. As can be seen in Fig. 3, reaction R1a occurs via TS1a by overcoming an energy barrier of 269.8 kJ/mol and 277.0 kJ/mol at G4 and CCSD(T)/cc-pV(T,Q)Z/MP2/cc-pVTZ levels of theory, respectively. TS1a is formed by stretching of the C-O ($r_{C\text{-}O}$ = 1.984 Å) and O-C ($r_{O\text{-}C}$ = 2.154 Å) bonds from their respective values ($r_{C\text{-}O}$ = 1.354 Å and $r_{O\text{-}C}$ = 1.435 Å) in the reactant molecule, and

View Article Online
DOI: 10.1039/C8SE00207J

simultaneously by an H-atom transfer. This reaction is an exothermic process ($\Delta_{r,0\ K}H^0$ = -37.7 and -34 kJ/mol at G4 and CCSD(T)/cc-pV(T,Q)Z/MP2/cc-pVTZ levels of theory, respectively). On the contrary, reaction R1b is endothermic, and unlike R1a, it retains the ring structure in the product after eliminating CO_2. Reaction R1b occurs via transition state TS1b which lies ~36 kJ/mol higher in energy than TS1a, and it does not involve an intramolecular H-transfer. However, in both transition states, C-O bonds being broken are elongated to about 2 Å to eventually release CO_2; whereas O-atom forming C-O bond ($r_{C\text{-}O}$ = 1.19 Å) in CO_2 moiety is found to be close to the final value of $r_{C\text{-}O}$ = 1.169 Å. We note here that the geometrical parameters of the transition states obtained at the MP2/cc-pVTZ and B3LYP/6-31G(2df,p) levels of theory show little method dependence. Not surprisingly, the calculated values of the barrier heights are found to be relatively low which indicate the concerted nature of these reactions. Reaction R2 proceeds via a four-center transition state TS2 by retaining the ring structure of the parent molecule to produce 4-methylene-1,3-dioxolan-2-one and H_2O. This reaction is also concerted in nature and occurs by overcoming an energy barrier of 304.5 kJ/mol. TS2 is found to be similar in structure to that observed by Kiecherer *et al.*[57] at MP2(FC)/cc-pVQZ level of theory for H_2O elimination in ethanol.

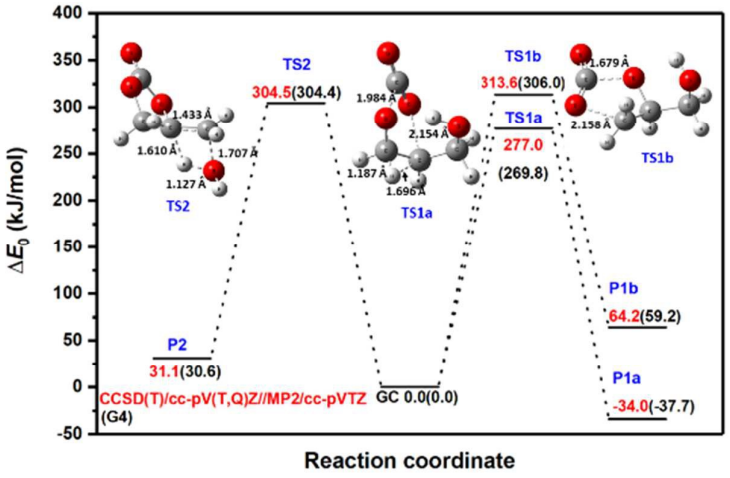

Figure 3. Zero-point corrected CCSD(T)/cc-pV(T,Q)Z//MP2-ccpVTZ energy profile for major channels of glycerol carbonate decomposition. G4 energies are also provided in the parentheses for comparison.

View Article Online
DOI: 10.1039/C8SE00207J

For the major channels (R1a, R1b and R2), G4 values were further refined at the CCSD(T)/CBS level of theory using extrapolations methods explained earlier. The results are provided in Fig. 3 and Table 1 for comparison. G4 method under-predicts the energies by ~7 kJ/mol for CO_2 elimination, whereas both methods predict the same barrier height for H_2O elimination pathway. Table 1 further compares the standard enthalpy of reaction ($\Delta_{r,298.15K}H^0$) obtained at various levels of theory. The different extrapolation schemes, namely Model 1, Model 2 and the Reference Model, predict very similar values for the standard enthalpy of reactions. The deviation given in parentheses is negligibly small with the largest deviation being 1.4 kJ/mol. Again, G4 values for standard enthalpy of reactions were found to be smaller than the Reference Model, HF/cc-pV(Q,5,6)Z + CCSD(T)/cc-pV(T,Q)Z. The energetics obtained by the Reference Model were used for RRKM/master equation calculations, and for the estimation of the highly accurate standard enthalpies of formation for the stable species at 0 K and 298.15 K using atomization scheme. The essential highly accurate atomization enthalpies were obtained from Ruscic's Active Thermochemical Tables (ATcT).[58]

Table 1. Standard enthalpy of reaction ($\Delta_{r,\ 298.15K}H^0$) obtained at various levels of theory for the major channels, i.e., R1a and R1b for CO_2 elimination and R2 for H_2O elimination. The deviations from the Reference Model (CCSD(T)/cc-pV(T,Q)Z//MP2/cc-pVTZ) are shown in parenthesis. The optimized geometries at the MP2/cc-pVTZ level of theory were used to obtain standard enthalpy of reaction at the CCSD(T) level of theory.

$\Delta_{r,298K}H^0$ kJ/mol	G4		Model 1		Model 2		Reference Model
			CCSD(T)/cc-pV(D,T)Z		CCSD(T)/cc-pV(T,Q)Z		CCSD(T)/cc-pV(T,Q)Z
			HF/cc-pV(D,T,Q)Z		HF/cc-pV(T,Q,5)Z		HF/cc-pV(Q,5,6)Z
R1a	-32.5	(-3.7)	-30.1	(-1.3)	-28.4	(0.3)	-28.8
R1b	63.1	(-5.0)	66.9	(-1.2)	68.3	(0.1)	68.1
R2	36.9	(-0.6)	38.3	(0.8)	37.1	(-0.4)	37.5

View Article Online
DOI: 10.1039/C8SE00207J

Reaction enthalpies usually are less dependent on the basis set, but the standard enthalpy of formation obtained by atomization scheme are more sensitive to the basis set used. We assess this dependency by computing single point energies at HF and CCSD(T) level of theory using various sizes of basis sets in the extrapolation schemes. We find that HF/cc-pV(Q,5,6)Z energy values are 4.3 kJ/mol lower than the extrapolated values obtained using cc-pV(T,Q,5)Z basis set. Further comparing to HF/cc-pV6Z energies, HF/cc-pV(Q,5,6)Z values are less by 0.3 kJ/mol. This clearly suggests that the final HF energies are not prone to any basis set dependency.

Table 2. Standard gas-phase enthalpy of formation values at 0 K ($\Delta_{f,0K}H^0$) and 298.15 K ($\Delta_{f,298.15K}H^0$) obtained from atomization scheme using Reference Model (CCSD(T)/cc-pV(T,Q)Z//MP2/cc-pVTZ).

Name	$\Delta_{f,0K}H^0$ (kJ/mol)	$\Delta_{f,298.15K}H^0$ (kJ/mol)	Ref.
Glycerol carbonate (GC)	-681.2	-702.9	This work
		-704.1	[59]
3-hydroxypropanal (P1a)	-325.4	-343.0	This work
Glycidol (P1b)	-227.1	-246.1	This work
	-218.3	-239.6	[60]
		-233.9	[61] G3MP2
4-methylene-1,3-dioxolan-2-one (P2)	-407.7	-420.6	This work

Based on the reference level of theory (HF/cc-pV(Q,5,6)Z + CCSD(T)/cc-pV(T,Q)Z//MP2/cc-pVTZ), standard enthalpies of formation were computed using the atomization scheme. Table 2 compiles and compares (wherever possible) standard enthalpies of formation ($\Delta_f H^0$) for glycerol carbonate and its decomposition products at 0 and 298.15 K.

View Article Online
DOI: 10.1039/C8SE00207J

As can be seen, our computed value of $\Delta_{f,298.15K}H^0$ = -702.9 kJ/mol for GC agrees very well with the value (-704.1 kJ/mol) reported by Ezhova *et al.*[59] who used Benson's group contribution method. As for glycidol (P1b), our value of $\Delta_{f,298.15K}H^0$ = -246.1 kJ/mol matches excellently with that reported in Burcat's database[60] ($\Delta_{f,298.15K}H^0$ = -239.6±8 kJ/mol). However, the value reported by Vasiliu[61] using G3MP2 level of theory shows a larger deviation of 12.2 kJ/mol. The origin of this discrepancy might be the inappropriately chosen conformer of glycidol (missing intramolecular hydrogen bond between OH group and O atom of oxirane). Vasiliu[61] also reported a value for the standard enthalpy of formation of 3-hydroxypropanal (P1a) ($\Delta_{f,298.15K}H^0$ = -327.6 kJ/mol), but this value appears to be for prop-2-en-1-ol. We confirmed this by checking the reported structure in the Supplementary Material of Ref. [61]. To the best of our knowledge, no other experimental and/or theoretical values for standard enthalpy of formation of 3-hydroxypropanal (P1a) and 4-methylene-1,3-dioxolan-2-one (P2) are available in the literature for comparison. Tables S1-S2 (Supplementary Materials) further compile the thermodynamics properties of the specie (GC, P1a, P1b and P2) in JANAF and NASA formats. Based on the calculated standard enthalpy of formation, the lower heating value (LHV) of glycerol carbonate is found to be 13.5 MJ/kg which is comparable to that of dimethyl carbonate (LHV = 15.8 MJ/kg)[14].

Theoretical Rate Coefficients. We obtained pressure- and temperature- dependence of the rate coefficients, $k(T,p)$, for the thermal decomposition of glycerol carbonate by solving thermal steady-state master equation using ChemRate[46]. These calculations used the parameters discussed in earlier section in addition to the vibrational frequencies and rotational constants listed in Table S3 (Supplementary Materials). We treat the low torsional mode as a vibration for both the reactant and the transition state. One can safely do so for OH rotors because their corresponding torsional frequencies are high (≥ 400 cm^{-1}). As for

View Article Online
DOI: 10.1039/C8SE00207J

(ring)C-CH_2OH hindered rotors in GC and transition states, we assume there will be systematic cancellation of errors. These torsional modes are identified as bold in Table S3 (Supplementary Materials). The calculated values of the rate coefficients, $k(T,p)$, for the three primary channels of GC decomposition are compiled in Table 3 and illustrated in Fig. 4 . Our calculated values of the rate coefficients, $k_{total}(T, p=1 \text{ atm})$, are close to the high pressure limiting rate coefficients, $k_{\infty,\text{total}}(T)$. Thus, GC displays negligible pressure dependence which is not surprising in view of its molecular size. For large molecules like GC, it is usual to observe $k(T, p) \approx k_{\infty}(T)$. For such molecular system, $k(E)$ drops rapidly below collisional stabilization rate $\beta k_s[M]$, *i.e.*, $\beta k_s[M] >> k(E)$ with bath gas M making no effect of pressure. Here, β and k_s are collision efficiency and collisional rate, respectively. However, the assumption $k(T,p) \approx k_{\infty}(T)$ may not be valid at high temperatures. For GC decomposition, we observed pressure fall off effect at high temperatures, e.g., $k_{\infty}(T)/k(T, p=1\text{atm}) / \approx 5$ at 2000 K.

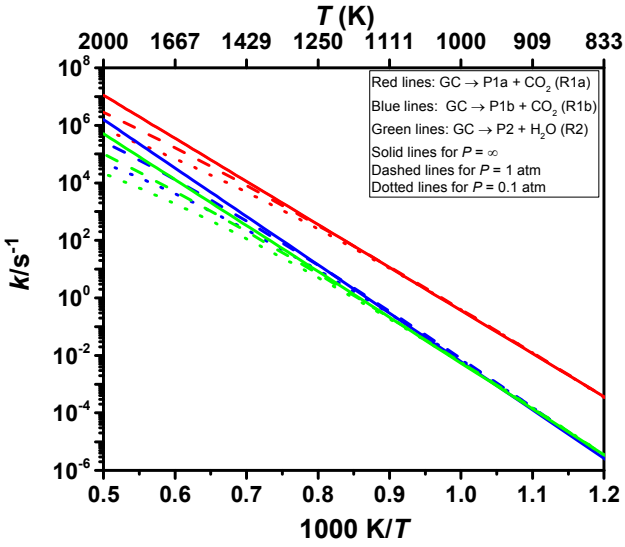

Figure 4. Arrhenius plots of the theoretical predictions of the rate coefficients of glycerol carbonate decomposition (GC). Red lines: GC → P1a + CO_2 (R1a); Blue lines: GC → P1b + CO_2 (R1b); Green lines: GC → P2 + H_2O (R2). Solid lines, dashed lines and dotted lines denote results for $p = \infty$, 1 atm and 0.1 atm, respectively.

View Article Online
DOI: 10.1039/C8SE00207J

Table 3. Calculated values for the pressure-dependent rate coefficients in the form of $k(T) = A\ T^n \exp(-E/RT)$ over the temperature range of 800 to 2000 K in units of J, mol, s, and K.

a) Rate parameters for reaction R1a: GC → P1a + CO_2

S. No.	*P* (atm)	Log(*A*)	*n*	*E*
1.	0.01	75.73	-18.05	421860
2.	0.1	59.46	-13.15	391014
3.	1	39.95	-7.40	347411
4.	10	23.59	-2.64	308207
5.	100	14.75	-0.075	286275
6.	∞	14.53	0	286561

b) Rate parameters for reaction R1b: GC → P1b + CO_2

S. No.	*P* (atm)	Log(*A*)	*n*	*E*
1.	0.01	88.82	-20.55	468569
2.	0.1	69.32	-16.05	446344
3.	1	48.53	-9.87	402664
4.	10	28.91	-4.14	356722
5.	100	17.30	-0.77	328208
6.	∞	14.61	0	322060

c) Rate parameters for reaction R2: GC → P2 + H_2O

S. No.	*P* (atm)	Log(*A*)	*n*	*E*
1.	0.01	76.93	-18.77	439467
2.	0.1	61.03	-13.92	411905
3.	1	40.23	-7.77	366796
4.	10	21.61	-2.33	322693
5.	100	10.94	-0.76	296372
6.	∞	13.68	0	305282

Among the three decomposition channels, reaction R1a is the most favored one contributing more than 85% in the entire temperature range (800 – 2000 K). This favoritism for the reaction can be attributed to the low value of the threshold energy (ΔE_0 = 277.0 kJ/mol) and also to an entropic gain ($\Delta_{298.15K}S^{\neq}$ = 47.6 J/mol K). Though R1b has a higher energy barrier

View Article Online
DOI: 10.1039/C8SE00207J

than that of R2 (see Fig. 3), it reacts faster than R1b which again can be explained from entropic insight. R1b is accompanied by an entropic gain ($\Delta_{298.15K}S^{\neq}$ = 60.4 J/mol K), whereas R2 occurs via a loss in entropy ($\Delta_{298.15K}S^{\neq}$ = -5.3 J/mol K) due to cyclization in the transition state structure. The transition state TS2 is tight as indicated by its imaginary frequency (ν = 1481.7*i*). Consequently, R2 contributes less than 4% over 800 – 2000 K, *i.e.,* CO_2 elimination makes the most contribution (≥ 96%) for GC decomposition over the entire temperature range of this study.

Similar to alkyl or aryl carbonates[62-64], GC also decomposes by utilizing two of its oxygen atoms to sequester just one carbon atom forming CO_2. Such oxygenates which dispense fuel-born oxygen to form CO_2 as opposed to CO have lesser propensity for soot reduction. For instance, alkyl or aryl carbonates having β-hydrogens decompose at appreciably low temperature via a low energy barrier of ≤ 200 kJ/mol [62] to produce olefin, CO_2 and alcohol, and their use as fuel additives has been found to be not more effective than alcohols for improving the threshold sooting index (TSI).[15] Hence, oxygenated fuel additives such as diethyl carbonate (DEC) do not have substantial effect in improving the sooting tendency. On the other hand, glycerol carbonate can potentially have higher propensity to reduce soot due to its decomposition to 3-hydroxypropanal and CO_2 exclusively. Despite the fact that two oxygen atoms in glycerol carbonate are wasted as CO_2, aldehydes, such as 3-hydroxypropanal, are reported to have the greatest impact to improve TSI.[15] The other reason being that the decomposition of alkyl and aryl carbonates is found to be almost three order of magnitude faster than that of GC below 1000 K. Consequently, even in low temperature oxidative environment (fuel/air mixtures), their unimolecular decomposition to produce alcohol, olefin and CO_2 still remains the predominant consumption pathways (see Ref. [65] for DEC low temperature oxidation). Therefore, the ignition behavior of such fuels is pretty

View Article Online
DOI: 10.1039/C8SE00207J

much governed by their decomposition products. Unlike other carbonates, glycerol carbonate is less reactive and can withstand higher temperatures ($t_{1/2}$ = 1.8 s at 1000 K). Because of its thermal stability, the reaction pathways for this molecule may drift towards abstraction reactions as opposed to molecular elimination reactions during low temperature oxidation. This expected drift in reaction mechanism for GC will possibly lead to a wide array of oxygenated intermediates that may have substantial impact on soot reduction. Therefore, glycerol carbonate appears to be more suitable compared to other oxygenated molecules for use as a fuel additive to reduce soot emissions.

Conclusions

Ab initio/RRKM-Master Equation calculations were performed to compute pressure- and temperature- dependence of the rate coefficients for glycerol carbonate (GC) decomposition. GC decomposes via a concerted mechanism almost exclusively to yield CO_2 and 3-hydroxypropanal. Carbon dioxide is the main decomposition product as in alkyl or aryl carbonates. CO_2 pathways contribute ≥ 96% to the total rate coefficient for GC decomposition. As expected, the unimolecular reaction of GC did not exhibit any pressure effect. Unlike alkyl or aryl carbonates, GC is found to be more thermally stable which can have a substantial effect on the spectrum of oxygenated intermediates formed during low temperature oxidation. As aldehydes are known to have the greatest impact on soot reduction among oxygenates, and 3-hydroxypropanal is one of the main products of GC decomposition, glycerol carbonate appears to have a high potential for use as a soot-reducing fuel additive.

Acknowledgements

Research reported in this work was funded by King Abdullah University of Science and Technology (KAUST). Milán Szőri acknowledges the support provided by the European Union and the Hungarian State, co-financed by the European Regional Development Fund in

View Article Online
DOI: 10.1039/C8SE00207J

the framework of the GINOP-2.3.4-15-2016-00004 project, aimed to promote the cooperation between the higher education and the industry. Milán Szőri is grateful for the financial support by the János Bolyai Research Scholarship of the Hungarian Academy of Sciences (BO/00113/15/7) and the New National Excellence Program of the Ministry of Human Capacities (ÚNKP-17-4-III-ME/26).

References

1. F. Fantozzi, A. Frassoldati, P. Bartocci, G. Cinti, F. Quagliarini, G. Bidini and E. M. Ranzi, *Applied Energy*, 2016, 184, 68-76.
2. P. Eastwood, *Critical topics in exhaust gas aftertreatment*, Research Studies Press, Baldock, Hertfordshire, 2001.
3. H. Chen, J. Wang, S. Shuai and W. Chen, *Fuel*, 2008, 87, 3462-3468.
4. N. Miyamoto, H. Ogawa, N. M. Nurun, K. Obata and T. Arima, SAE Technical Paper 980506, 1998, https://doi.org/10.4271/980506.
5. H. Teng and J. C. McCandless, SAE Technical Paper 2006-01-0053, 2006, https://doi.org/10.4271/2006-01-0053.
6. C. A. G. Quispe, C. J. R. Coronado and J. A. Carvalho Jr, *Ren. Sust. Energ. Rev.*, 2013, 27, 475-493.
7. A. Rodrigues, J. C. Bordado and R. G. d. Santos, *Energies*, 2017, **10**, 1817.
8. M. Pagliaro, R. Ciriminna, H. Kimura, M. Rossi and C. Della Pina, *Angew. Chem. Int. Edit.*, 2007, 46, 4434-4440.
9. W. A. Khanday, P. U. Okoye and B. H. Hameed, *Energy Conversion and Management*, 2017, **151**, 472-480.
10. M. O. Sonnati, S. Amigoni, E. P. Taffin de Givenchy, T. Darmanin, O. Choulet and F. Guittard, *Green Chem.,* 2013, **15**, 283-306.
11. J. R. Ochoa-Gómez, O. Gómez-Jiménez-Aberasturi, C. Ramírez-López and M. Belsué, *Org. Process Res. Dev.*, 2012, 16, 389-399.
12. J. R. Ochoa-Gómez, O. Gómez-Jiménez-Aberasturi, B. Maestro-Madurga, A. Pesquera-Rodríguez, C. Ramírez-López, L. Lorenzo-Ibarreta, J. Torrecilla-Soria and M. C. Villarán-Velasco, *Appl. Catal. A: General*, 2009, 366, 315-324.
13. M. Kozak, J. Merkisz, P. Bielaczyc and A. Szczotka, *SAE International*, 2009.
14. P. Rounce, A. Tsolakis, P. Leung and A. P. E. York, *Energy & Fuels*, 2010, 24, 4812-4819.
15. P. Pepiot-Desjardins, H. Pitsch, R. Malhotra, S. R. Kirby and A. L. Boehman, *Combus. Flame*, 2008, 154, 191-205.
16. Y. Ren, Z. Huang, H. Miao, Y. Di, D. Jiang, K. Zeng, B. Liu and X. Wang, *Fuel*, 2008, 87, 2691-2697.
17. B. Sirjean, P. A. Glaude, M. F. Ruiz-Lopez and R. Fournet, *J. Phys. Chem. A*, 2006, 110, 12693-12704.
18. J. H. Kiefer, K. S. Gupte, L. B. Harding and S. J. Klippenstein, *J. Phys. Chem. A*, 2009, 113, 13570-13583.

View Article Online
DOI: 10.1039/C8SE00207J

19. F. Zhang, Z. D. Wang, Z. H. Wang, L. D. Zhang, Y. Y. Li and F. Qi, *Energy Fuels*, 2013, 27, 1679-1687.
20. A. Lucassen, Z. Wang, L. Zhang, F. Zhang, W. Yuan, Y. Wang, F. Qi and K. Kohse-Höinghaus, *Proc. Combust. Inst.*, 2013, 34, 641-648.
21. M. Verdicchio, B. Sirjean, L. S. Tran, P.-A. Glaude and F. Battin-Leclerc, *Proc. Combust. Inst.*, 35, 533-541.
22. X. Yang, A. W. Jasper, B. R. Giri, J. H. Kiefer and R. S. Tranter, *Phys. Chem. Chem. Phys.*, 2011, 13, 3686-3700.
23. L. A. Curtiss, P. C. Redfern and K. Raghavachari, *J. Chem. Phys.*, 2007, 126, 084108.
24. H. P. Hratchian and H. B. Schlegel, *J. Chem. Phys.* 2004, 120, 9918-9924.
25. H. P. Hratchian and H. B. Schlegel, *J. Chem. Theory Comput.*, 2005, 1, 61-69.
26. A. D. Becke, *Phys. Rev. A*, 1988, 38, 3098-3100.
27. P. J. Stephens, F. J. Devlin, C. F. Chabalowski and M. J. Frisch, *J. Phy. Chem.*, 1994, 98, 11623-11627.
28. C. Møller and M. S. Plesset, *Phys. Rev*, 1934, 46, 618-622.
29. C. Møller and M. S. Plesset, *Phys Rev*, 1934, **46**, 618-622.
30. R. A. Kendall, T. H. Dunning and R. J. Harrison, *J. Chem. Phys.*, 1992, 96, 6796.
31. J. P. Merrick, D. Moran and L. Radom, *J. Phys. Chem. A*, 2007, 111, 11683-11700.
32. G. D. Purvis and R. J. Bartlett, *J. Chem. Phys.*, 1982, 76, 1910-1918.
33. G. E. Scuseria, C. L. Janssen and H. F. Schaefer, *J. Chem. Phys.*, 1988, 89, 7382.
34. G. E. Scuseria and H. F. Schaefer, *J. Chem. Phys.*, 1989, 90, 3700.
35. L. Masgrau, A. n. González-Lafont and J. M. Lluch, *J. Chem. Phys.*, 2001, 115, 4515.
36. R. Izsak, M. Szori, P. J. Knowles and B. Viskolcz, *J. Chem. Theory Comput.*, 2009, 5, 2313-2321.
37. B. R. Giri, F. Khaled, M. Szőri, B. Viskolcz and A. Farooq, *Proc. Combust. Inst.,* 2017, 36, 143-150.
38. M. AlAbbad, B. R. Giri, M. Szőri and A. Farooq, *Proceedings of the Combustion Institute*, 2017, 36, 187-193.
39. T. Helgaker, W. Klopper, H. Koch and J. Noga, *J. Chem. Phys.*, 1997, 106, 9639-9646.
40. T. H. Dunning, *J. Chem. Phys.*, 1989, 90, 1007.
41. D. Feller, *J. Chem. Phys.*, 1992, 96, 6104-6114.
42. T. H. Dunning, *J. Chem. Phys.*, 1989, 90, 1007-1023.
43. D. E. Woon and T. H. Dunning, *J. Chem. Phys.*, 1993, 98, 1358-1371.
44. T. J. Lee and P. R. Taylor, *Int. J. Quantum Chem.*, 1989, 199-207.
45. M. J. Frisch, G. W. Trucks, H. B. Schlegel, G. E. Scuseria, M. A. Robb, et al. Gaussian 09 Revision D.01., Gaussian Inc., Wallingford CT, 2009.
46. Vladimir Mokrushin, V. B., Wing Tsang, Michael R. Zachariah, Vadim D. Knyazev, W. Sean McGivern *ChemRate*, 1.5.8; NIST: Gaithersburg, USA, 2011.
47. R. G. Gilbert and S. C. Smith, *Theory of Unimolecular and Recombination Reactions*, Blackwell Scientific Publications, 1990.
48. T. Baer and W. L. Hase, *Unimolecular Reaction Dynamics: Theory and Experiments*, Oxford University Press, 1996.
49. P. J. Robinson and K. A. Holbrook, *Unimolecular Reactions*, Wiley-Interscience, 1972.
50. T. Beyer and D. F. Swinehart, *Commun. ACM*, 1973, 16, 379.
51. C. Eckart, *Phys. Rev.*, 1930, 35, 1303-1309.
52. H. S. Johnston and J. Heicklen, *J. Phys. Chem.*, 1962, 66, 532-533.
53. A. M. Zaras, P. Dagaut and Z. Serinyel, *J. Phys. Chem. A*, 2015, 119, 7138-7144.
54. A. M. Zaras, S. Thion and P. Dagaut, *Int. J. Chem. Kinet.* 2015, 47, 439-446.

View Article Online
DOI: 10.1039/C8SE00207J

55. M. Akbar Ali and A. Violi, *J. Org. Chem.*, 2013, 78, 5898-5908.
56. H. Hippler, J. Troe and H. Wendelken, *J. Chem. Phys.*, 1983, 78, 6709-6717.
57. J. Kiecherer, C. Bansch, T. Bentz and M. Olzmann, *Proc. Combust Inst.*, 2015, 35, 465-472.
58. B. Ruscic, R. E. Pinzon, M. L. Morton, G. von Laszevski, S. J. Bittner, S. G. Nijsure, K. A. Amin, M. Minkoff and A. F. Wagner, *J. Phys. Chem. A*, 2004, 108, 9979-9997.
59. N. N. Ezhova, I. G. Korosteleva, N. V. Kolesnichenko, A. E. Kuz'min, S. N. Khadzhiev, M. A. Vasil'eva and Z. D. Voronina, *Petrol Chem+*, 2012, 52, 91-96.
60. E. Goos, A. Burcat and B. Ruscic, *Extended Third Millennium Ideal Gas and Condensed Phase Thermochemical Database for Combustion with Updates from Active Thermochemical Tables*. 16 July 2016 ed.; 2016.
61. M. Vasiliu, K. Guynn and D. A. Dixon, *J. Phys. Chem. C*, 2011, 115, 15686-15702.
62. M. AlAbbad, B. R. Giri, M. Szori, B. Viskolcz and A. Farooq, *Chem. Phys. Lett.*, 2017, 684, 390-396.
63. H. O'Neal and S. Benson, *J. Phys. Chem.*, 1967, 71, 2903-2921.
64. J. Cross, R. Hunter and V. Stimson, *Aus. J. Chem.*, 1976, 29, 1477-1481.
65. H. Nakamura, H. J. Curran, A. Polo Córdoba, W. J. Pitz, P. Dagaut, C. Togbé, S. M. Sarathy, M. Mehl, J. R. Agudelo and F. Bustamante, *Combust. Flame*, 2015, 162, 1395-1405.

View Article Online
DOI: 10.1039/C8SE00207J

A Table of Contents Entry

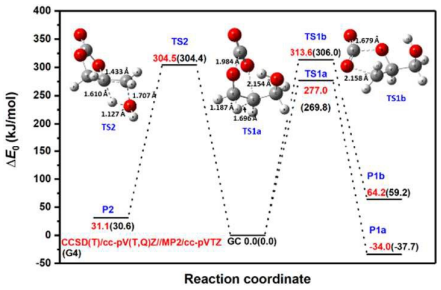

Glycerol carbonate can be a promising fuel or a promising soot-reducing fuel additive for sustainable future.